Stress Analysis Method for Clearance-Fit Joints with Bearing-Bypass Loads

Rajiv A. Naik*
Analytical Services and Materials, Inc., Hampton, Virgina
and
John H. Crews Jr.†
NASA Langley Research Center, Hampton, Virginia

In multi-fastener joints, fastener holes may be subjected to combined bearing loads and bypass loads that are reacted elsewhere in the joint. The analysis of a joint with such loading is complicated by the usual clearance between the hole and the fastener. A simple analysis method for clearance-fit joints with bearing-bypass loading is presented in this paper. This analysis uses an inverse formulation and can be implemented with most general purpose finite element programs. A quasi-isotropic graphite/epoxy plate was analyzed with a rigid, frictionless bolt. Computed results showed that the contact angle and the peak stresses at the hole were strongly influenced by the bearing-bypass stress ratio. Tension and compression bearing-bypass loading had opposite effects on the contact angle. For large compressive bearing-bypass loads, the hole tended to close on the fastener leading to dual contact. Dual contact reduced the stress concentration at the fastener and would, therefore, increase joint strength. The results illustrate the general importance of accounting for bolt-hole clearance and contact to accurately compute bolt-hole stresses.

Nomenclature

c	= radial clearance, m
c_d	= diametrical clearance, %
d	= hole diameter, m
E_1	= modulus in fiber direction, GPa
E_2	= modulus transverse to fiber, GPa
G_{12}	= shear modulus, GPa
P	= applied load, N
P_b	= bearing load, N
P_{bp}	= bypass load, N
r,θ	= polar coordinates, m, deg
r_b	= bolt radius, m
R	= hole radius,
S_b , S_b^*	= nominal bearing stress, MPa
S_{np}	= nominal net-section bypass stress, MPa
t	= specimen thickness, m
u,v	= x and y displacements, m
w	= specimen width, m
x,y	= Cartesian coordinates, m
β	= bearing-bypass ratio, S_b/S_{np}
θ_1, θ_2	= bolt-hole contact angle, deg
ν_{12}	= Poisson's ratio
σ	= stress component, MPa
σ_{rr}	= radial stress component, MPa
$\sigma_{\theta\theta}$	= tangential stress component, MPa

Presented as Paper 89-1230 at the AIAA 30th AIAA/ASME/ASCE/AHS/ASC Structures, Structural Dynamics, and Materials Conference, April 3-5, 1989; received Aug. 28, 1989; revision received and accepted for publication April 18, 1990.

*Research Scientist.
†Senior Engineer, Materials Division.

Introduction

AEROSPACE structures are commonly fabricated using mechanically fastened joints. To better understand the complex behavior of such joints, it is important to develop accurate stress analysis methods. This is especially important for composite structures, since they can be seriously weakened by fastener holes and often have rather complex failure modes. Within a multifastener structural joint, fastener holes may be subjected to the combined effects of bearing loads and loads that bypass the hole, as illustrated in Fig. 1. The ratio of bearing load to bypass load depends on the joint stiffness and configuration.

The combined effects of bearing and bypass loads can be simulated by testing and analyzing single-fastener specimens (Fig. 1). However, very little research has been published on the stress analysis of single-fastener specimens subjected to combined bearing and bypass loading. In 1981, Ramkumar[1] and Soni[2] used a two-dimensional finite element stress analysis to determine the stress state around the fastener in a single-fastener laminate subjected to bearing-bypass loads. The fastener load was modeled by imposing zero radial displacements

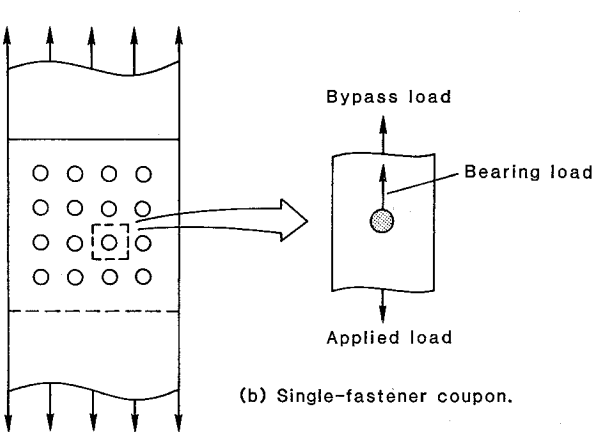

Fig. 1 Bearing-bypass loading within a multifastener joint.

on the load-carrying half of the fastener hole. In the same year, Garbo[3] used his BJSFM analysis to obtain the stresses in a single-fastener laminate subjected to bearing-bypass loads. This analysis is based on the anisotropic theory of elasticity in conjunction with laminated plate theory. It assumes a loaded and unloaded hole in an infinite domain, and uses the principle of superposition in conjunction with the appropriate elasticity stress functions. The fastener load was simulated by specifying a radial stress boundary condition varying as a cosine over half the hole.

In almost all practical applications, some clearance exists between the hole and the fastener. The presence of a clearance leads to a contact region at the bolt-hole interface that varies nonlinearly with the load and influences the stress state around the hole. Although this nonlinearity complicates the analysis, it is important to make an accurate stress analysis to better understand the complex failure modes. Futhurmore, for some combinations of compressive bearing-bypass loads, the hole tends to close in on the fastener leading to "dual contact." The effects of clearance have been presented in Refs. 4-9.

The objective of the present paper is, first, to present a simple, direct stress analysis method for a laminate with a clearance-fit fastener subjected to combined bearing and bypass loads in tension or compression, including dual contact, and, then, to study the effects of bearing-bypass loads on bolt-hole contact and local stresses. The present approach uses a linear-elastic finite element analysis with an inverse formulation like that in Refs. 4–6. Conditions along the bolt-hole interface are specified by constraint equations that limit nodal displacements to a circular arc corresponding to the bolt diameter. These equations describe the contact conditions more realistically than the distributions usually assumed for radial displacement[1,2,7,10] or stress.[3] Furthermore, the present technique does not need an iterative-incremental method of solution, which usually involves tedious node tracking along the contact arc.[11-14] The finite element analysis was performed using the MSC/NASTRAN computer code.[15] The material properties used in the analysis represent a quasi-isotropic T300/5208 graphite/epoxy laminate. The bolt was assumed to be rigid and the interface to be frictionless.

Results are presented as curves relating the nominal bearing stress and the bolt-hole contact angle for various combinations of bearing and bypass loads. Also, the effect of bypass load on the bolt-hole contact angle is presented for constant bearing loads. Hole boundary stresses for a range of bearing-bypass load proportions in both tension and compression are also presented for a typical bearing load level. Finally, a solution array for a range of bearing-bypass loads, typical load-contact variations, and local stresses are presented for dual-contact situations.

Analysis

The configuration and loading analyzed in the present study is shown in Fig. 2 for a typical tension bearing-bypass case. The gross applied load P is reacted partly in bearing P_b and partly as a bypass load P_{bp} at the other end of the model. The nominal bearing stress S_b and net-section bypass stress S_{np} are defined as shown in Fig. 2. The bolt was assumed to be rigid and the bolt-hole interface to be frictionless. The diametrical clearance c_d between the hole and the bolt was expressed as a percentage of the hole diameter d. The material represented in the analysis was a quasi-isotropic T300/5208 graphite/epoxy laminate with the following properties: E = 59.46 GPa and G = 20.4 GPa. Isoparametric, quadrilateral, and triangular elements were used to model the laminate.[4,15] Nodes were placed every 0.9375 deg along the hole boundary to model the contact angles accurately. Loads P and P_{bp} were applied to the ends of the model. The desired bearing-bypass ratio β was obtained by an appropriate choice of P and P_{bp}.

For a snug-fit joint (c_d = 0), the contact angle θ_1 along the bolt-hole interface does not vary with S_b, and a simple linear stress analysis can be used. However, for a clearance-fit joint ($c_d > 0$), the contact angle θ_1 increases nonlinearly with S_b, as shown in Fig. 3. This nonlinear load-contact variation at the bolt-hole interface greatly complicates the stress analysis. Bypass loads also influence the nonlinear load-contact variation, further complicating the analysis for combined bearing-bypass loading.

Inverse Formulation

The nonlinear load-contact variation shown in Fig. 3 could be accounted for in an iterative incremental scheme in which the nominal bearing stress S_b is incremented in small steps and the corresponding contact angle θ_1 is determined iteratively at each load step. Such a procedure would require special purpose finite element programming, and also would involve tedious node tracking along the contact arc.[11-14] Alternatively, an inverse technique[4] can be used in which a contact angle θ_1 is assumed and the corresponding bearing stress S_b is computed by a simple procedure described later. The inverse technique is simple to use because the boundary conditions for an assumed contact angle θ_1 are fixed and known at the outset. For an assumed contact angle, the contact problem is linear, and the analysis procedure can be repeated for a range of contact angles to determine a nonlinear load-contact curve like that in Fig. 3. Therefore, although the contact problem is nonlinear, the inverse technique requires only linear finite element analyses; linear NASTRAN procedures were used to solve this nonlinear problem. As previously mentioned, the conditions along the bolt-hole interface were specified by displacement constraint equations. The formulation of these constraint equations and the solution procedures are described in the following two sections.

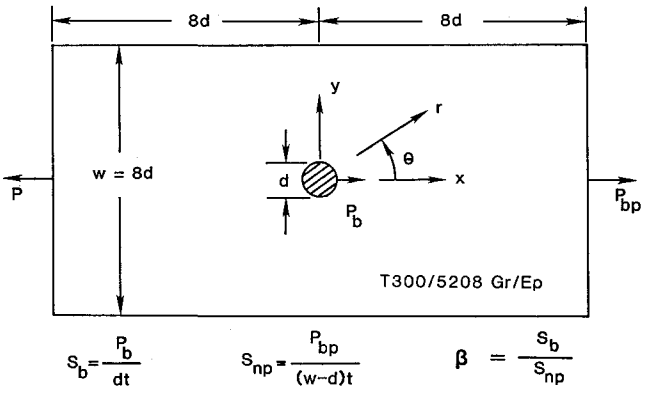

Fig. 2 Plate configuration for bearing-bypass loading.

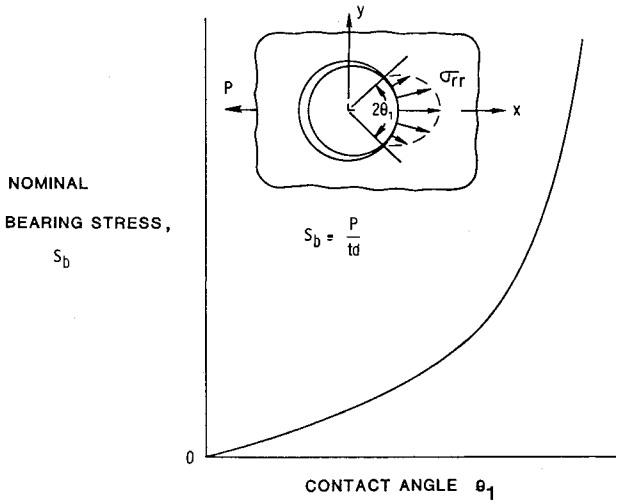

Fig. 3 Nonlinear relationship between bearing stress and contact angle.

Displacement Constraint Equations

Figure 4 shows the analysis model for a typical case of contact at the bolt-hole interface. The bolt radius r_b is smaller than the hole radius R by the amount of radial clearance c. To simplify the analysis, the bolt is assumed to be fixed in space, and the orgin of the reference coordinate system is located at the center of the undeformed hole. Before load is applied, contact occurs only at point A. After the model is loaded on the two ends by P and P_{bp}, points along the hole boundary that lie within an assumed contact arc AB contact the frictionless surface of the fixed rigid bolt.

Consider a point $P(x,y)$ on the hole boundary within the assumed contact arc AB (see Fig. 4). Let u and v be the x and y displacements necessary to move point P from its original position to a point on the surface of the bolt. The deformed position of P may be described by the following equation:

$$[(x - c) + u]^2 + [y + v]^2 = r_b^2 \tag{1}$$

By expressing x and y in polar coordinates, neglecting the higher order u and v terms, and noting that $r_b = R - c$, Eq. (1) may be rewritten as follows:

$$A\,u + B\,v = C \tag{2}$$

where

$$A = R\cos\theta - c \tag{3}$$

$$B = R\sin\theta \tag{4}$$

and

$$C = R\,c(\cos\theta - 1) \tag{5}$$

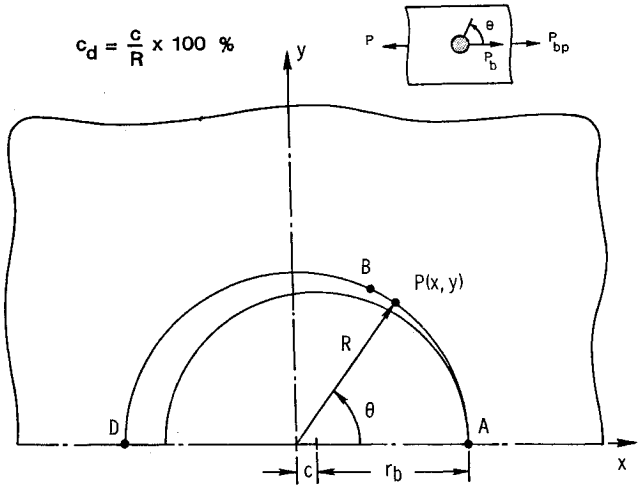

Fig. 4 Hole clearance notation for single-sided contact.

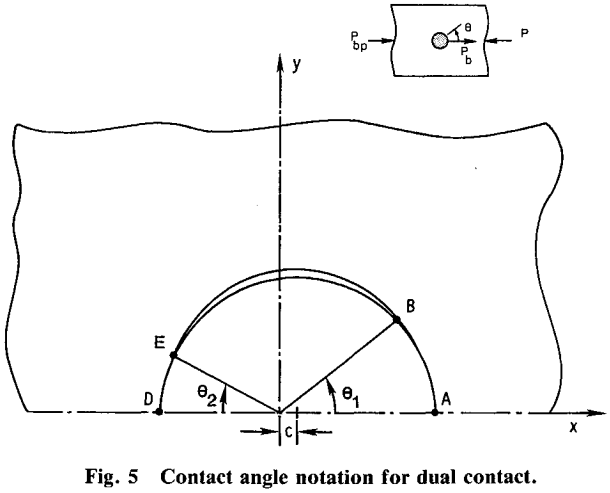

Fig. 5 Contact angle notation for dual contact.

Equation (2) is a constraint equation for the u and v displacements of any point $P(x,y)$ on the contact arc AB. The quantities A, B, and C can be computed at the outset, since they are functions of the initial geometry. In the finite element analysis, the displacements of each node within the contact region can be specified by applying Eq. (2) as a multipoint contraint.[13] Note that the hole boundary beyond the contact arc is stress free. This fact will be used later in the analysis.

As mentioned earlier, for some compression bearing-bypass loads, the hole tends to close on the bolt, leading to dual contact at the bolt-hole interface. For example, point D on the hole boundary in Fig. 4 could move in the positive x direction and make contact with the bolt surface. This would correspond to the onset of dual contact. Further loading would lead to dual contact, as shown in Fig. 5. The contact angles θ_1 and θ_2 for dual contact would also, in general, vary nonlinearly with load. However, the inverse technique can also be used for dual contact. Multipoint constraints, as described by Eq. (2), can be used to specify nodal displacements within the two contact regions. The corresponding combination of bearing and bypass loads can then be determined by the solution procedure described later.

Solution Procedure for Single Contact

The correct bearing stress S_b for an assumed contact angle θ_1 was established using a simple procedure and the NASTRAN computer code. Point A (Fig. 4), which was assumed to be in contact with the rigid bolt, was fixed. Displacements of all nodes within the assumed contact arc were restricted to those allowed by the multipoint constraints given by Eq. (2). Thus, all the boundary conditions, including those along the bolt-hole interface, are defined. However, since the contact angle θ_1 and the nominal bearing stress S_b are nonlinearly related, the correct S_b corresponding to the assumed θ_1 is still unknown.

For a specified θ_1, the problem is linear and, thus, the stresses in the plate are linearly related to S_b and S_{np}. A linear equation relating σ_{rr}, S_b, and S_{np} can be written as

$$\sigma_{rr}(r,\theta) = F_1(r,\theta)\,S_b + F_2(r,\theta)\,S_{np} + F_3(r,\theta) \tag{6}$$

where F_1, F_2, and F_3 are constants for a given r and θ. The first two terms in this equation represent the σ_{rr} components, due to the applied bearing and bypass loads, respectively. The third term represents the σ_{rr}, due to imposing the multipoint constraints, and is a function of clearance, as indicated by Eqs. (2-5).

For given bearing-bypass ratio β, we can write S_{np} as

$$S_{np} = S_b/\beta \tag{7}$$

Substituting Eq. (7) into Eq.(6) gives

$$\sigma_{rr}(r,\theta) = F_4(r,\theta)\,S_b + F_3(r,\theta) \tag{8}$$

where

$$F_4(r,\theta) = F_1(r,\theta) + F_2(r,\theta)/\beta \tag{9}$$

The hole boundary region beyond the contact angle θ_1 is stress free. Thus,

$$\sigma_{rr}(R,\theta) = 0 \qquad \theta_1 \le \theta \le \pi \tag{10}$$

This stress boundary condition was imposed at the end of the contact arc as

$$\sigma_{rr}(R,\theta_1) = 0 \tag{11}$$

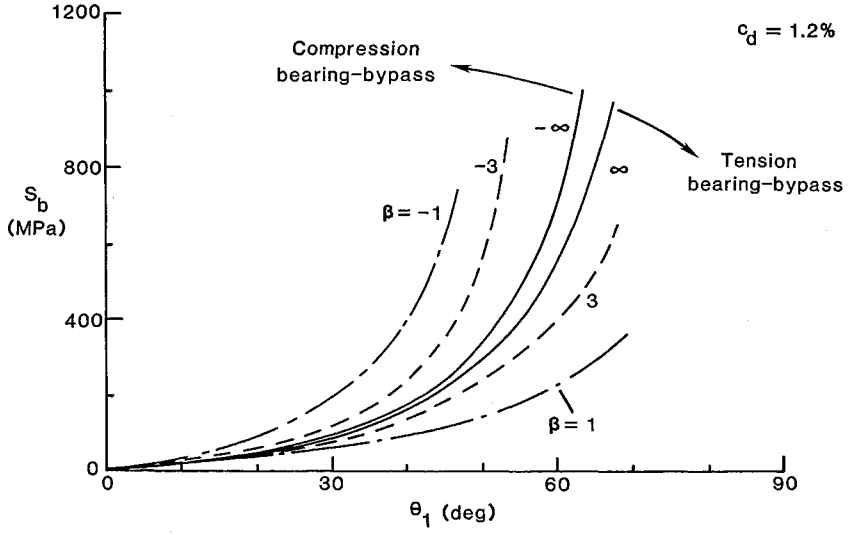

Fig. 6 Effect of bearing-bypass ratio on load-contact relationship.

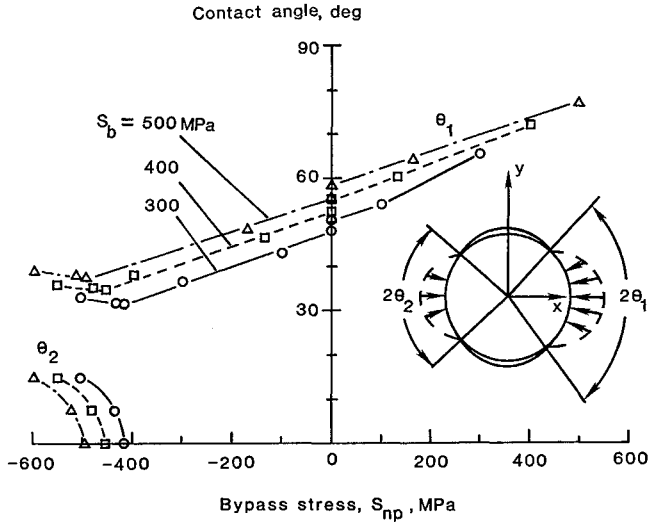

Fig. 7 Variation of contact angle with bypass stress.

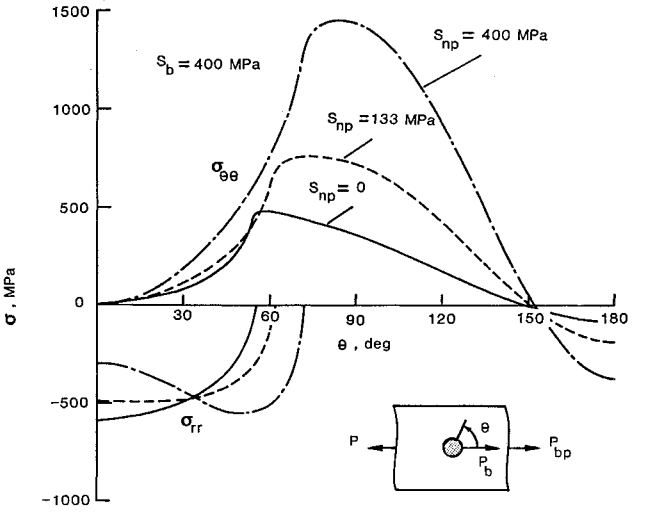

Fig. 8 Stresses along hole boundary for tension loading.

If S_b^* is the correct bearing stress for an assumed contact angle θ_1, then from Eqs. (8) and (11), we have the following relation:

$$F_4(R,\theta_1)\, S_b^* + F_3(R,\theta_1) = 0 \tag{12}$$

This equation can be rewritten as follows:

$$S_b^* = -F_3(R,\theta_1) / F_4(R,\theta_1) \tag{13}$$

For a given β, the values of $F_3(R,\theta_1)$ and $F_4(R, \theta_1)$ were determined by the following procedure. For an assumed θ_1, the stress S_b was selected arbitrarily, and σ_{rr} was calculated at the end of the contact arc using a finite element analysis. These S_b and σ_{rr} values were then used in Eq. (8) to get one equation for $F_3(R,\theta_1)$ and $F_4(R, \theta_1)$. A second S_b was selected (arbitrarily), and again the corresponding σ_{rr} at the end of the contact was calculated. The second set of S_b and σ_{rr} values was used in Eq. (8) to get a second equation for $F_3(R,\theta_1)$ and $F_4(R,\theta_1)$. The two equations were solved simultaneously to determine $F_3(R,\theta_1)$ and $F_4(R,\theta_1)$, which were used in Eq. (13) to find S_b^*. This procedure was repeated for a series of assumed θ_1 values to determine the corresponding S_b^* values. These pairs of θ_1 and S_b^* values can then be plotted to establish S_b vs θ_1 curves for single contact in the clearance-fit joint. The preceding procedure was introduced and evaluated in Ref. 4. It can be successfully applied for both tension and compression bearing-bypass loads that lead to single contact. A slightly different procedure, described in the next section, is used for dual contact.

Solution Procedure for Dual Contact

As described earlier, compression bearing-bypass loads may cause dual contact at the bolt. The dual contact angles θ_1 and θ_2 (see Fig. 5) increase nonlinearly with load. However, for specified θ_1 and θ_2, the stresses in the plate are linearly related to S_b , S_{np}, and the bolt-hole contact stresses associated with the imposed multipoint constraints. A linear equation relating σ_{rr}, S_b, and S_{np} can be written for the end of each contact arc. For point B (see Fig. 5),

$$\sigma_{rr}(R,\theta_1) = K_1(R,\theta_1)\, S_b + K_2(R,\theta_1)\, S_{np} + K_3(R,\theta_1) \tag{14}$$

and for point E,

$$\sigma_{rr}(R, \pi - \theta_2) = K_4(R, \pi - \theta_2) S_b + K_5(R, \pi - \theta_2) S_{np} + K_6(R, \pi - \theta_2) \tag{15}$$

The constants K_1-K_6 are similar to those in Eq. (6). Again, the first two terms in both Eqs. (14) and (15) represent the σ_{rr} components, due to the bearing and bypass loads, respectively. The third term represents the σ_{rr} associated with the imposed multipoint constraints. Equations (14) and (15) cannot be simplified further using Eq. (7), as was done earlier for the single-contact case [see Eqs. (6) and (8)], because the bearing-bypass ratio β that would lead to contact angles θ_1 and θ_2 is not known a priori. The constants K_1-K_3 and K_4-K_6 can be determined by calculating $\sigma_{rr}(R,\theta_1)$ and $\sigma_{rr}(R,\pi-\theta_2)$ for three different (arbitrary) combinations of S_b and S_{np}. The calculated stresses and the corresponding values of S_b and S_{np} are then substituted into Eqs. (14) and (15) to yield three equations in K_1, K_2, and K_3 and three equations in K_4, K_5, and K_6. These six equations are solved simultaneously to determine K_1-K_6. Now the correct values of S_b and S_{np} corresponding to the assumed θ_1 and θ_2 values can be determined by imposing the boundary conditions at the ends of the contact arcs as $\sigma_{rr}(R,\theta_1) = 0$ and $\sigma_{rr}(R,\pi-\theta_2) = 0$. Substituting these boundary conditions into Eqs. (14) and (15), we have

$$K_1(R,\theta_1)S_b + K_2(R,\theta_1)\,S_{np} + K_3(R,\theta_1) = 0 \qquad (16)$$

$$K_4(R,\pi-\theta_2)\,S_b + K_5(R,\pi-\theta_2)\,S_{np} + K_6(R,\pi-\theta_2) = 0 \qquad (17)$$

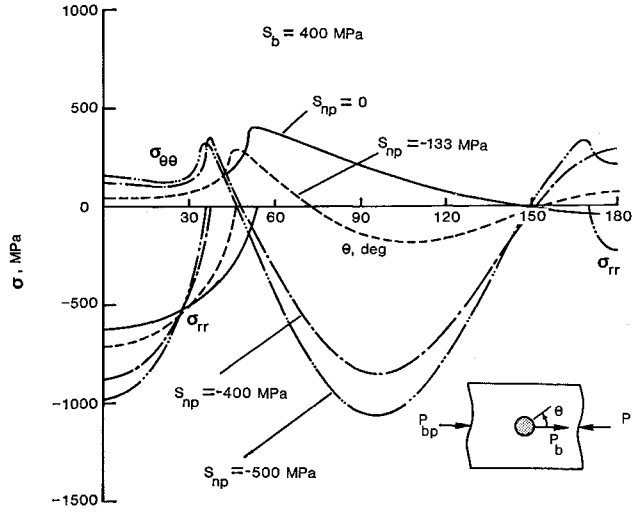

Fig. 9 Stresses along hole boundary for compression loading.

The only unknowns in the preceding equations are S_b and S_{np}, which can be determined by the simultaneous solution of Eqs. (16) and (17). The preceding procedure can be repeated for different sets of assumed contact angles θ_1 and θ_2 to determine the corresponding S_b vs S_{np} plot, as discussed in the following section.

Results and Discussion

All of the results in this paper were obtained for the finite-size plate shown in Fig. 2 with a clearance c_d of 1.2%. First, results are presented for single contact with both tension and compression bearing-bypass loads. Next, the effect of bypass loading on bolt-hole contact is shown for a constant bearing loading. The corresponding hole boundary stresses are also presented. Results are then presented for dual contact. Contact angles are presented on an S_b vs S_{np} plot, and local stresses are presented for a dual-contact case.

Single Contact

The effect of bearing-bypass ratio β on the bearing stress-contact angle curves is shown in Fig. 6 for single contact. Note that $\beta = \infty$ corresponds to a tension bearing case with no bypass load, and $\beta = -\infty$ represents the corresponding compression bearing case. The bearing-bypass ratio β was found to have a considerable effect on the bearing stress-contact angle behavior. For tension bearing-bypass at a bearing stress level of 400 MPa, a typical bearing strength for graphite/epoxy, the contact angle (Fig. 6) for $\beta = 1$ is about 30% larger than that for $\beta = \infty$. In compression bearing-bypass at $S_b = 400$ MPa, the contact angle for $\beta = -1$ is about 25% smaller than that for $\beta = -\infty$.

The variation of contact angle with bypass stress is shown in Fig. 7 for three S_b levels. Increasing the tensile bypass loading resulted in an increased θ_1, whereas increasing the compressive bypass loading had the opposite effect. The small jog in the curve at $S_{np} = 0$ is caused by the small difference between tension-reacted bearing and compression-reacted bearing. For the $S_b = 400$ MPa case, dual contact initiated for a compressive bypass stress of about 450 MPa. The secondary contact angle θ_2 increased rather abruptly as the compressive S_{np} exceeded this value. Additionally, the decreasing trend for θ_1 reversed when dual contact developed.

For $S_b = 400$ MPa, the tangential ($\sigma_{\theta\theta}$) and radial (σ_{rr}) stresses around the hole boundary are shown in Fig. 8 for three different values of S_{np} for tension bearing-bypass loading. The peak value of the σ_{rr} stress is not very sensitive to S_{np}.

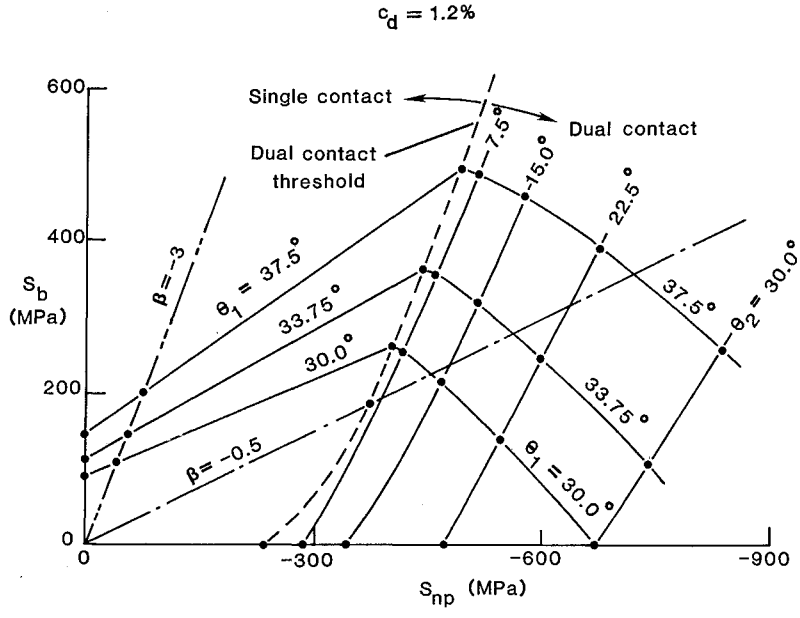

Fig. 10 Solution array for dual contact.

The σ_{rr} peak usually occurs at 0 deg for small values of S_{np}. However, the distribution of σ_{rr} changes with increased S_{np} values, showing the increased contact angle, as in Fig. 7. For $S_{np} = 400$ MPa, the σ_{rr} peak occurs at around 55 deg. The increase in the peak $\sigma_{\theta\theta}$ stresses rises nearly proportionally with the increase in S_{np} stress. The location of the peak $\sigma_{\theta\theta}$ is usually a few degrees beyond the contact region. The location of the $\sigma_{\theta\theta}$ peak is important because damage in composite joints often starts at this location.[5]

The $\sigma_{\theta\theta}$ and σ_{rr} hole boundary stresses for compressive S_{np} stresses are shown in Fig. 9. For $S_{np} = 0$ ($\beta = -\infty$), $\sigma_{\theta\theta}$ is mostly tensile. For $S_{np} = -133$ MPa, $\sigma_{\theta\theta}$ becomes compressive in the net-section (around 90 deg) of the joint. For $S_{np} = -400$ MPa, the compression peak of $\sigma_{\theta\theta}$ is larger and more of the hole boundary is in compression. Unlike the tension bearing-bypass cases, the peak value of the σ_{rr} stress in compression bearing-bypass increases nearly proportionally with the bypass load and always occurs at $\theta = 0$ deg. For example, the peak σ_{rr} stress for $S_{np} = 400$ MPa is 40% higher than the $S_{np} = 0$ case. The $S_{np} = 500$ MPa case results in dual contact at the hole, as indicated by the σ_{rr} stress for $\theta > 170$ deg. The $\sigma_{\theta\theta}$ stress for this case shows tensile peaks at the end of each of the two contact regions.

Dual Contact

The S_b and S_{np} values calculated for assumed values of θ_1 and θ_2 are plotted in Fig. 10. Each solid circular symbol represents a solution corresponding to assumed contact angles θ_1 and θ_2. The dashed curve represents the onset of dual contact. The region to the right of the dashed curve represents the dual-contact region. The double-dashed line represents the $\beta = -3$ case. Note that this line runs almost parallel to the linear portion of the dual-contact threshold line (dashed line), indicating that the $\beta = -3$ case would never involve dual contact. Thus, dual contact would occur only when $-3 < \beta \leq 0$. The dashed-dot line represents the $\beta = -0.5$ case. It intersects the dual-contact curve (dashed) at $S_{np} = -375$ MPa. Thus, dual contact for this case would begin at $S_{np} = -375$ MPa ($S_b = 187.5$ MPa). Note that all results in Fig. 10 were obtained for a clearance of 1.2% of hole diameter. A smaller clearance would cause dual contact to develop at a lower load level and vice versa.

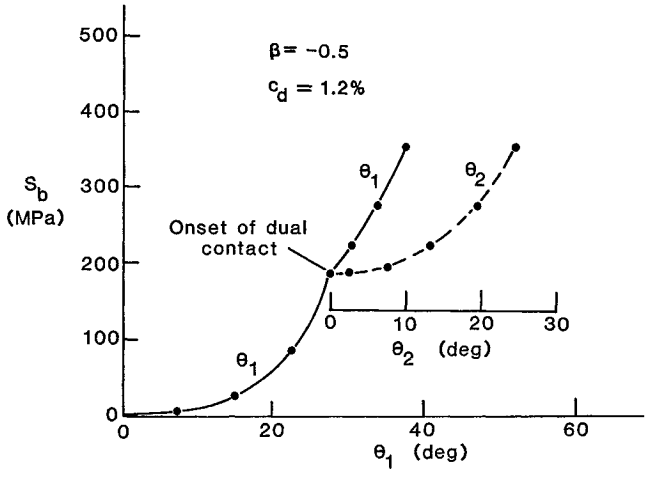

Fig. 11 Effect of dual contact on S_b vs θ relationship.

The effect of dual contact on the S_b vs θ_1 curve is shown in Fig. 11. The S_b vs θ_1 curve before dual contact was generated using the procedure for single-contact analysis described earlier. The remainder of the curve was constructed from Fig. 10 by selecting S_b, θ_1, and θ_2 values on the $\beta = -0.5$ line. Some interpolation was used. The S_b vs θ_1 relationship changes after the onset of dual contact. The S_b vs θ_2 curve is also nonlinear and θ_2 increases more rapidly than θ_1 with increasing load.

An important consequence of dual contact is that it allows load transfer across the bolt and, therefore, reduces the stress concentration around the fastener hole. Figure 12 illustrates this effect by comparing hole boundary stresses for a case with dual contact to stresses for an open hole case at the same load level. The peak $\sigma_{\theta\theta}$ for the open hole case is 13% higher than that for the dual-contact case. This suggests that dual contact is advantageous, since it reduces stresses around the hole and increases the joint strength. Smaller bolt-hole clearances promote dual contact and, therefore, should produce higher joint strengths in compression.

Concluding Remarks

A simple method has been developed for the stress analysis of a laminate with a clearance-fit fastener subjected to combined bearing and bypass loading in tension or compression, including dual-contact situations. This method uses a linear elastic finite element analysis with an inverse formulation. The present method is simple to apply and can be implemented with most general purpose finite element programs. The method was applied to study the effects of bearing-bypass load proportioning on the bolt-hole contact angles and local stresses. The initial clearance between the smooth rigid bolt

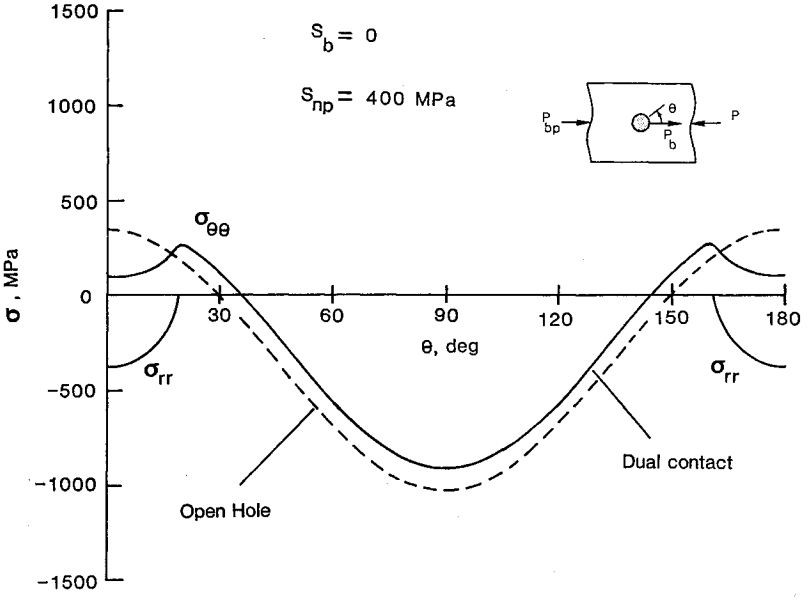

Fig. 12 Effect of dual contact on hold boundary stresses.

and the hole was 1.2% of the hole diameter in all analyses. Material properties for the plate represented a quasi-isotropic graphite/epoxy laminate. The bearing-bypass proportions were expressed in terms of β, the ratio of bearing stress S_b to bypass stress S_{np}.

The bearing-bypass ratio β was found to have a considerable effect on the nonlinear contact behavior. Under tension bearing-bypass with $S_b = 400$ MPa, the contact angle was 30% larger for $\beta = 1$ than that for $\beta = \infty$. Compressive bypass loading had the opposite effect: the contact angle was 25% smaller for $\beta = -1$ than that for $\beta = -\infty$ at $S_b = 400$ MPa. For single-contact situations under tension bearing bypass, the peak tangential stresses around the hole boundary increased proportionately with the S_{np} stress. The peak radial stress was not very sensitive to S_{np}. However, under compressive bearing-bypass loading, both the peak tangential and peak radial stresses were considerably influenced by S_{np}. For β greater than -3, the hole tended to close on the fastener leading to dual contact. Dual contact allows load transfer across the fastener and, therefore, reduces the stress concentration around the hole. Dual contact, therefore, has a beneficial effect on the joint strength.

These results illustrate the general importance of accounting for bolt-hole clearance and contact to accurately compute local bolt-hole stresses for combined bearing and bypass loading.

References

[1]Ramkumar, R. L., "Bolted Joint Design, Test Methods and Design Allowables for Fibrous Composites," American Society for Testing and Materials, ASTM STP 734, edited by C. C. Chamis, 1981, pp. 376–395.

[2]Soni, S. R., "Stress and Strength Analysis of Bolted Joints in Composite Laminates," *Composite Structures*, edited by I. H. Marshall, Applied Science Publishers, London, 1981, pp. 50–62.

[3]Garbo, S. P., and Ogonowski, J. M, "Effect of Variances and Manufacturing Tolerances on the Design Strength and Life of Mechanically Fastened Composite Joints," *Methodology Development and Data Evaluation*, AFWAL-TR-81-3041, Vols. 1–3, April 1981.

[4]Naik, R. A. and Crews, J. H., Jr., "Stress Analysis Method for a Clearance-Fit Bolt Under Bearing Loads," *AIAA Journal*, Vol. 24, Aug. 1986, pp. 1348–1353.

[5]Crews, J. H., Jr., and Naik, R. A., "Failure Analysis of a Graphic/Epoxy Laminate Subjected to Bolt Bearing Loads," *Composite Materials: Fatigue and Fracture, ASTM STP 907*, edited by H. T. Hahn, American Society for Testing Materials, Philadelphia, PA, 1986, pp. 115–133; also NASA TM-86297, Aug. 1984.

[6]Crews, J. H., Jr., and Naik, R. A., "Combined Bearing and Bypass Loading on a Graphite/Epoxy Laminate," *Composite Structures*, Vol. 6, Nos. 1–3, 1986, pp. 21–40; also NASA TM-87705, April 1986.

[7]Oplinger, D. W., and Gandhi, K. R., "Stresses in Mechanically Fastened Orthtropic Laminates," *Proceedings of the Second Conference on Fibrous Composites in Flight Design*, AFFDL-TR-74-103, Sept. 1974, pp. 813–841.

[8]DeJong, T., "The Influence of Friction on the Theoretical Strength of Pin-Loaded Holes on Orthotropic Plates," Delft Univ. of Technology, Delft, the Netherlands, Rept. LR-350, March 1982.

[9]Eshwar, V. A., "Analysis of Clearance Fit Pin Joints," *International Journal of Mechanical Sciences*, Vol. 20, Aug. 1978, pp. 477–484.

[10]Mongalgiri, P.D., Dattaguru, B., and Rao, A. K., "Finite Element Analysis of Moving Contact in Mechanically Fastened Joints," *Nuclear Engineering Design*, Vol. 78, April 1984, pp. 303–311.

[11]Francavilla, A., and Zienkiewicz, O.C., "A Note on Numerical Computation of Elastic Contact Problems," *International Journal for Numerical Methods in Engineering*, Vol. 9, Sept. 1975, pp. 913–924.

[12]White, D. J., and Enderby, L. R., "Finite Element Stress Analysis of a Nonlinear Problem: A Connecting-Rod Eye Loaded by Means of a Pin," *Journal of Strain Analysis*, Vol. 5, No. 1, 1970, pp. 41–48.

[13]Sholes, A., and Strover, E. M., "The Piecewise-Linear Analysis of Two Connecting Structures Including the Effect of Clearance at the Connections," *International Journal for Numerical Methods in Engineering*, Vol. 3, Jan. 1971, pp. 45–51.

[14]Chan, S. K., and Tuba, I. S., "A Finite Element Method for Contact Problems of Solid Bodies—Part I. Theory and Validation," *International Journal of Mechanical Sciences*, Vol. 13, May 1971, pp. 615–625.

[15]*MSC/NASTRAN, User's Manual, Vol. 1 and 2,* The MacNeal-Schwendler Corp., Los Angeles, CA, MSR-39, Nov. 1985.